A Discretized Population Balance for Nucleation, Growth, and Aggregation

The population balance for batch aggregation of particulate suspensions is recast in a form that may be solved simply and accurately. The transformed equation is deduced with the introduction of only one additional parameter, which is found to be a constant for all cases. The transformed equation is tested by comparison with some analytical solutions with which it is found to be in excellent agreement. In particular, the equation is shown to predict correctly the rate of change of total particle number and volume. Compatible descriptions of linear growth and nucleation are developed with similar success.

The method is then applied to modeling the *in vitro* growth and aggregation of kidney stones (calcium oxalate monohydrate crystals). It is found that these phenomena are well described by McCabe's ΔL law, a size-independent coalescence kernel, and first-order kinetics. Simulated particle size distributions and their moments are in excellent agreement with the experimental results.

M. J. Hounslow
Department of Chemical Engineering
University of Adelaide
Adelaide, South Australia 5001

R. L. Ryall, V. R. Marshall
Urology Unit, Department of Surgery
Flinders Medical Centre
Bedford Park, South Australia, 5042

Introduction

The mathematical description of a system of particles simultaneously undergoing nucleation, growth, and aggregation produces an equation that is entirely intractable analytically for all but the most idealized situations. In seeking a solution to such an equation one is essentially searching for a description of how the particles are distributed by size and by time. The solution, in the rare cases that it is available, effectively describes with infinite precision this functional relationship. Such a degree of precision is usually far from justified; in simulation studies the underlying kinetic parameters are seldom known with any great accuracy, and in the analysis of experimental size distributions, information is generally available only for a finite number of discrete size intervals.

The lack of analytical solutions necessitates the use of numerical techniques in which the particle size domain is discretized into a large number of intervals, typically more than 30, and any of a number of integration methods applied (Gelbard and Seinfield, 1978; Ramkrishna, 1985). The results of these techniques are sufficiently detailed, by the criteria given above, but the computational requirements are substantial.

An alternative technique used by Batterham et al. (1981) and Marchal et al. (1988) is to discretize the particle size domain into as many intervals as is convenient, frequently using a $\sqrt[3]{2}$ geometric progression, and to replace the integrals with summations. The computational requirements are substantially diminished, to the extent that a desktop microcomputer frequently may be used. The results produced contain sufficient detail in most instances but incorporate systematic errors in the prediction of total particle number and volume.

The objective of the current work is the development of a numerical technique for the simulation of batch, *in vitro* kidney stone formation trials. In these trials, seeds of calcium oxalate monohydrate (COM) grow and aggregate in a supersaturated solution of calcium oxalate. The role of linear growth under the influence of a supersaturation driving force is clear and well established as a mechanism for the formation of urinary stones. Much less clear, but possibly more important, is the role of aggregation in this process. Aggregation has the potential to produce very large, and consequently harmful, crystals in a short period of time with no relief of supersaturation.

The data from the batch trials may be examined in a qualitative way by observation of total crystal number and volume; number is conserved by growth and volume by aggregation. Some quantitative conclusions may be drawn using the numerical technique of Ryall et al. (1986) in which the "*extents*" of growth and of aggregation over some time interval are calculated. The technique uses first-order numerical integration and requires that the ratio of the extents be constant from one time interval to the next. A trial and error technique is used to choose the best-fit values of the extents. As well as being extremely

cumbersome computationally, the technique does not produce the underlying kinetic parameters.

In what follows, the population balance technique is applied to develop a mathematical description for the system under consideration; particular attention is paid to the value of using moments in such a description. In order to avoid the very heavy computational complexity associated with the aggregation term, the prospect of discretization is introduced. Discretized equations are developed for the description, in turn, of aggregation, growth, and nucleation. As each equation is developed it is tested against a number of analytical solutions. The solution of these equations is simple and very fast, even on a microcomputer. The *in vitro* formation of urinary stones is explored as a case study.

Theory

Population balances

The population balance, or particle number continuity equation, for a well-mixed batch system of constant volume is given by Randolph and Larson (1971, p. 49) as

$$\frac{\partial n}{\partial t} + \frac{\partial (Gn)}{\partial L} = B - D \tag{1}$$

In this equation, n is the number-density function: If in the system there are dN particles per unit volume of suspension in the size range L to $L + dL$, then at that size and time the density function is $n = dN/dL$. Equation 1 relates the rate of change of number of particles in the differential size range L to $L + dL$, to the rates of growth into and out of that range and the rates of birth and death in the size range.

In writing the population balance as Eq. 1, only growth, of the three phenomena of interest, appears explicitly. Before considering how appropriate birth and death functions might be formed for the other phenomena, a small simplification may be made to the growth term. The McCabe ΔL law (McCabe, 1929) states that the growth rate is not a function of length and thus, for growth only, Eq. 1 reduces to

$$\frac{\partial n}{\partial t} = -G\frac{\partial n}{\partial L} \tag{2}$$

Nucleation. The nucleation rate B_0 is taken to be the rate of appearance of particles of zero size, from which it follows that

$$B = B_0 \delta(L) \tag{3}$$

where $\delta(L)$ is the Dirac delta function

Aggregation. Hulburt and Katz (1964) developed a population balance model for aggregation using volume as the internal coordinate. The model has found extensive use in the description of agglomeration in balling circuits, particularly for iron ore (Kapur and Fuerstenau, 1969; Sastry, 1975; Batterham et al. 1981). For aggregation alone the birth and death rates are

$$B'(v) = \frac{1}{2}\int_0^v \beta'(v-\epsilon, \epsilon)\, n'(v-\epsilon)\, n'(\epsilon)\, d\epsilon \tag{4}$$

$$D'(v) = n'(v)\int_0^\infty \beta'(v, \epsilon)\, n'(\epsilon)\, d\epsilon \tag{5}$$

The prime is used to signify volume as the internal coordinate. The coalescence kernel, $\beta'(v, \epsilon)$, is a measure of the frequency of collisions between particles of volumes v and ϵ that are successful in producing a particle of volume $v + \epsilon$.

The ease with which growth may be described using length as the internal coordinate provides the motivation for seeking to convert Eqs. 4 and 5 to a length-based form:

$$B(L) = \frac{L^2}{2}\int_0^L \frac{\beta[(L^3-\lambda^3)^{1/3}, \lambda]\, n[(L^3-\lambda^3)^{1/3}]\, n(\lambda)\, d\lambda}{(L^3-\lambda^3)^{2/3}} \tag{6}$$

$$D(L) = n(L)\int_0^\infty \beta(L, \lambda)\, n(\lambda)\, d\lambda \tag{7}$$

Moment transforms

Randolph and Larson (1971, p. 53) have given a clear appraisal of the virtues of using moments in the solution of population balance problems. In general the application of initial conditions and auxiliary equations to the population balance results in a set of integro-partial-differential equations of mixed dimension, for which analytical solutions can rarely be found. The moment transform can frequently be used to convert this intractable set of equations into a set of ordinary differential equations.

The jth moment is defined as

$$m_j = \int_0^\infty L^j n(L)\, dL \tag{8}$$

The first four moments are of particular interest; they are related to total number, length, area, and volume of solid per unit volume of suspension by

$$N_T = m_0 \tag{9a}$$

$$L_T = k_L m_1 \tag{9b}$$

$$A_T = k_A m_2 \tag{9c}$$

$$V_T = k_V m_3 \tag{9d}$$

The values of the shape factors depend on the shape of the particles and the type of particle size analyzer being used. For a Coulter Counter $k_V = \pi/6$ irrespective of particle shape while the analysis of spheres on that device requires $k_L = 1$, $k_A = \pi$.

Nucleation and Growth. Randolph and Larson (1971, p. 57) show that for nucleation and growth alone, under the conditions of interest here, the moments may be generated by the ordinary differential equation

$$\frac{dm_j}{dt} = 0^j B_0 + jGm_{j-1} \tag{10}$$

Aggregation. Application of Eq. 8 to the population balance, Eq. 1, for the case of zero growth rate, yields

$$\frac{dm_j}{dt} = \overline{B}_j - \overline{D}_j \tag{11}$$

where

$$\overline{B_j} = \int_0^\infty L^j B \, dL \tag{12}$$

$$\overline{D_j} = \int_0^\infty L^j D \, dL \tag{13}$$

Applying Eq. 12 to Eq. 6 we have

$$\overline{B_j} = \int_0^\infty \frac{L^{2+j}}{2} \cdot \int_0^L \frac{\beta[(L^3 - \lambda^3)^{1/3}, \lambda] \, n[(L^3 - \lambda^3)^{1/3}] n(\lambda)}{(L^3 - \lambda^3)^{2/3}} \, d\lambda \, dL \tag{14}$$

Similarly, Eq. 7 becomes

$$\overline{D_j} = \int_0^\infty L^j n(L) \int_0^\infty \beta(L, \lambda) n(\lambda) \, d\lambda \, dL \tag{15}$$

Further simplification of Eqs. 14 and 15 is not possible without some knowledge of the form of the coalescence kernel. If the coalescence kernel is not a function of particle size, then putting $u^3 = L^3 - \lambda^3$ and reversing the order of integration, Eq. 14 becomes

$$\overline{B_j} = \frac{\beta_0}{2} \int_0^\infty n(\lambda) \int_0^L (u^3 + \lambda^3)^{j/3} n(u) \, du \, d\lambda \tag{16}$$

Equation 16 may be expanded in terms of a closed set of moments [i.e., $\overline{B_j} = \overline{B_j}(m_k : k \le j)$] only if $j/3$ is an integer. Consequently, of the first four moments, only the zero and the third may be described in this way.

$$\overline{B_0} = \frac{1}{2} \beta_0 m_0^2 \tag{17}$$

$$\overline{B_3} = \beta_0 m_0 m_3 \tag{18}$$

For death by aggregation, with a size-independent coalescence kernel, Eq. 15 becomes

$$\overline{D_j} = \beta_0 \int_0^\infty L^j n(L) \int_0^\infty n(\lambda) \, d\lambda \, dL = \beta_0 m_0 m_j \tag{19}$$

Combining Eqs. 11, 17, 18, and 19

$$\frac{dm_0}{dt} = -\frac{1}{2} \beta_0 m_0^2 \tag{20}$$

$$\frac{dm_3}{dt} = 0 \tag{21}$$

Equations 20 and 21 are entirely in agreement with those produced directly by Hulburt and Katz (1964) from Eqs. 4 and 5 using volume as the internal coordinate.

Discretization

In generating discrete equations to replace the foregoing continuous population balances a number of points need to be borne in mind. How accurate need the results be, and indeed which results are of most importance? For instance, are minor errors in the prediction of particle size distribution (PSD) tolerable provided the moments can be predicted correctly? If the total number and volume of solids is to be used to fit kinetic parameters then this last question can be answered in the affirmative. If however, a comparison of predicted and experimental PSD's is to be used to infer the validity of a kinetic model, a different conclusion may be drawn.

In what follows, substantial emphasis is placed on determining whether both the moments and the PSD are predicted correctly.

Discretization for Aggregation

The motivation for discretizing the population balance equations arises solely out of the difficulty incurred by the inclusion of the aggregation terms given in Eqs. 6, 7, 15, and 16. The direct solution of equations containing these terms by use of conventional finite difference techniques is complicated by the presence of the integral term and results in a computational load far greater than is desirable.

Previous work

Batterham et al. (1981) have proposed a set of discretized equations describing the process of aggregation. Using volume as the internal coordinate they first considered the case in which the particle size domain is divided into intervals of equal value so that $v_{i+1} - v_i$ is a constant. As the authors pointed out, covering even a modest range of particle sizes results in a very large range of volumes. As a consequence, virtually no information is conveyed about the smaller sizes if a manageable number of size increments is to be maintained.

Batterham et al. then considered a discretized size domain in which volumes were in a geometric series such that $v_{i+1}/v_i = 2$. Considering the PSD as a truly discrete distribution—that is, only particles of size v, $2v$, $4v$, etc. exist—they deduced equations that allowed interaction of particles at the appropriate rate and split the particles so formed into the permissible sizes in such a way as to conserve volume. For example, particles of size v and $2v$ interact to form a single particle of size $3v$, however $3v$ is not a permissible size. The closest permissible sizes are $2v$ and $4v$, so to conserve volume, half a particle of size $2v$ is formed and half a particle of size $4v$ is formed. The resulting equation is

$$\frac{dN_i}{dt} = \frac{3}{8} \beta_{i-2,i-1} N_{i-2} N_{i-1} + \frac{3}{4} \beta_{i-1,i} N_{i-1} N_i + \beta_{i-1,i-1} N_{i-1}^2 + \sum_{j=1}^{i-2} (1 + 2^{j-i}) \beta_{i,j} N_i N_j - \sum_j \beta_{i,j} N_i N_j - \beta_{i,i} N_i^2 \tag{22}$$

In order to calculate moments from data of this type, Eq. 8 must be rewritten in a discrete form:

$$m_j = \sum_i \overline{L_i^j} N_i \tag{23}$$

where $\overline{L_i^j}$ is the appropriate mean size in the ith interval for calculating the jth moment. The calculation of this mean is considered later.

It follows from Eq. 23 that

$$\frac{dm_j}{dt} = \sum_i \overline{L_i^j} \frac{dN_i}{dt} \tag{24}$$

By application of Eq. 24 to Eq. 22, expressions may be deduced for the rate of change of the moments. For the case of a size-independent coalescence kernel, ($\beta_{i,j} = \beta_0$) the results may be compared with Eqs. 20 and 21. Consider the rate of change of the zero moment:

$$\begin{aligned}\frac{dm_0}{dt} &= \sum_i \frac{dN_i}{dt} \\ &= \sum_i \frac{3}{8}\beta_0 N_{i-2}N_{i-1} + \sum_i \frac{3}{4}\beta_0 N_{i-1}N_i + \sum_i \beta_0 N_{i-1}^2 \\ &\quad + \sum_i \sum_{j-1}^{i-2} (1 + 2^{j-i})\beta_0 N_i N_j - \sum_i \sum_j \beta_0 N_i N_j - \sum_i \beta_0 N_i^2 \\ &= \sum_i \beta_0 N_i \left(\frac{9}{8} N_{i-1} + \sum_{j-i}^{i-2} 2^{j-1} N_j - \sum_{j-i-1}^{i-2} N_j\right)\end{aligned}$$

which cannot be reconciled with Eq. 20.

Turning now to the rate of change in the third moment and noting that $\overline{L_{i+1}^3} = 2\overline{L_i^3}$:

$$\begin{aligned}\frac{dm_3}{dt} &= \sum_i \overline{L_i^3} \frac{dN_i}{dt} \\ &= \sum_i \frac{3}{8}\beta_0 \overline{L_{i+1}^3} N_{i-1}N_i + \sum_i \frac{3}{4}\beta_0 \overline{L_i^3} N_{i-1}N_i \\ &\quad + \sum_i \beta_0 \overline{L_{i+1}^3} N_i^2 + \sum_i \sum_{j-1}^{i-2} (1 + 2^{j-i})\beta_0 \overline{L_i^3} N_i N_j \\ &\quad - \sum_i \sum_j \beta_0 \overline{L_i^3} N_i N_j - \sum_i \beta_0 \overline{L_i^3} N_i^2 \\ &= \sum_i \beta_0 \overline{L_i^3} N_i \\ &\quad \cdot \left[\frac{3}{2} N_{i-1} + N_i + \sum_{j-1}^{i-2} (1 + 2^{j-i}) N_j - \sum_j N_j\right] \\ &= \sum_i \beta_0 \overline{L_i^3} N_i \left(\sum_{j-1}^{i-1} 2^{j-i} N_j - \sum_{j-i+1}^{\infty} N_j\right) \\ &= \beta_0 \left(\sum_i \sum_{j-1}^{i-1} \overline{L_j^3} N_i N_j - \sum_i \sum_{j-i+1}^{\infty} \overline{L_i^3} N_i N_j\right)\end{aligned} \tag{25}$$

It can be shown that the two summation terms in Eq. 25 are identical, so $dm_3/dt = 0$, which is the required result, Eq. 21, deduced from the continuous moment equations.

In summary, the approach of Batterham et al. treats particle volume appropriately, guaranteeing its conservation. However, the rate of change of particle numbers using their equations is not predicted correctly. Such a result is not surprising given the arbitrary allocation of particle numbers used in the generation of their equations.

A new approach

Before proceeding to develop a new model for aggregation it is worth reflecting on the nature of the length-domain discretization to be used. There are two immediate reasons for choosing a geometric discretization in which $L_{i+1}/L_i = \sqrt[3]{2}$. First, as Batterham et al. remark, it enables a great range of sizes to be covered in a useful fashion. Second, it corresponds exactly to the discrete output of the Coulter Counter. A further advantage is that it is useful in developing the new model of aggregation because particles can aggregate into a given size interval only if one of the particles, prior to forming an aggregate, was in the size interval immediately smaller than the interval of interest. Further, should an aggregate be formed by particles both from the same interval it will always be of such a size as to be counted in the next interval. Such a combination of practical and theoretical arguments makes the discretization discussed here the obvious choice; it is used throughout this work.

Table 1. Binary Interaction Mechanisms for Aggregation

Mechanism	Birth or Death in Interval i	Collisions between Particles in Intervals	
1	Birth	$i-1$	$1 \rightarrow i-2$
2	Birth	$i-1$	$i-1$
3	Death	i	$1 \rightarrow i-1$
4	Death	i	$i \rightarrow \infty$

The model

A technique is required for generating an equation, possibly similar to Eq. 22, that deals correctly with the rate of change of particle number and volume. For mathematical convenience four binary interaction mechanisms are considered, as displayed in Table 1.

Assume that the particle size distribution may be represented by the idealized density function shown in Figure 1b. The internal coordinate used is volume, the domain being divided into intervals in a geometric series such that the smallest size in the ith interval is 2^i and the largest size is 2^{i+1}. (Size in this context is measured by particle volume rather than length.) The density function in this interval is given by $n' = N_i/2^i$.

Mechanism **1.** Birth in the ith interval can occur only when a particle in the $(i-1)$th interval aggregates with a particle in the first to $(i-1)$th) intervals. Consider the aggregation of a particle of size a in the jth interval, where $j < i-1$. In order to form a particle in the ith interval it must collide with particles in the size range $2^i - a \le v < 2^i$, all of which are in the $(i-1)$th)

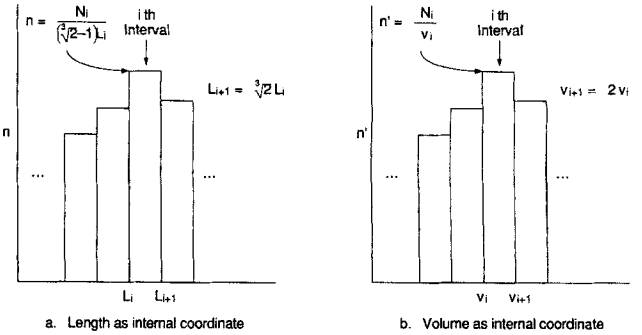

Figure 1. Discrete size distributions with length or volume as internal coordinate.

interval. The number of particles available for collision is thus $aN_{i-1}/2^{i-1}$.

The differential rate of aggregation by this first mechanism, $dR^{[1]}$, for particles in the size range $a < v < a + da$ (of which there are dN), resulting in particles in the ith interval is given by

$$dR_{i,j}^{[1]} = \beta \frac{aN_{i-1}}{2^{i-1}} dN$$

$$= \beta \frac{aN_{i-1}}{2^{i-1}} n'(a)da$$

$$= \beta \frac{aN_{i-1}}{2^{i-1}} \frac{N_j}{2^j} da$$

Thus, allowing that $\beta = \beta_{i-1,j}$ for particles in the $(i-1)$th and jth intervals:

$$R_{i,j}^{[1]} = \beta_{i-1,j} \int_{2^j}^{2^{j+1}} a2^{1-i-j} N_{i-1} N_j \, da$$

$$= 3 \cdot 2^{j-i} \beta_{i-1,j} N_{i-1} N_j$$

$R_{i,j}^{[1]}$ is the rate of birth in the ith interval resulting from aggregation between particles in the jth interval by the first mechanism. If this rate is summed over all possible values of j, the total rate of birth in the ith interval by the first mechanism may be determined:

$$R_i^{[1]} = \sum_{j=1}^{i-2} 3 \cdot 2^{j-i} \beta_{i-1,j} N_{i-1} N_j \tag{26}$$

Mechanism **2.** A similar process may be used for aggregates formed in the ith interval by collisions between particles both in the $(i-1)$th interval. Any aggregate formed by a collision between a particle in the $(i-1)$th interval and another particle in the same interval will result in the formation of a particle in the ith interval, consequently the number of particles available is N_{i-1}, and the differential rate of birth is

$$dR_i^{[2]} = \frac{1}{2} \beta_{i-1,i-1} N_{i-1} \frac{N_{i-1}}{2^{i-1}} da$$

The leading factor of $1/2$ is included to avoid counting collisions twice.

$$R_i^{[2]} = \beta_{i-1,i-1} \int_{2^{i-1}}^{2^i} \frac{N_{i-1}^2}{2^i} da$$

$$= \frac{1}{2} \beta_{i-1,i-1} N_{i-1}^2 \tag{27}$$

Mechanism **3.** Death by aggregation will occur to a particle in the ith interval should it collide and adhere to a particle of sufficient size for the resultant aggregate to be larger than the upper size limit of the ith interval.

First, consider collisions with particles from smaller size ranges. Death in the ith interval will occur when a particle of size a, in the jth interval, aggregates with a particle ranging in size from $2^{i+1} - a$ to 2^{i+1}. The number of particles in this latter range is $aN_i/2^i$.

The rates may be calculated as before:

$$R_{i,j}^{[3]} = 3 \cdot 2^{j-i-1} \beta_{i,j} N_i N_j$$

By summing this last equation over all feasible values of j, death by the third mechanism may be reckoned:

$$R_i^{[3]} = N_i \sum_{j=1}^{i-1} 3 \cdot \beta_{i,j} 2^{j-i-1} N_j \tag{28}$$

Mechanism **4.** If a particle in the ith interval aggregates with a particle from that or a higher interval, a death occurs in the ith interval. This final mechanism may be quantified simply as

$$R_i^{[4]} = N_i \sum_{j=i}^{\infty} \beta_{i,j} N_j \tag{29}$$

The overall rate of change of numbers may be computed by collecting the terms of Eqs. 26 to 29:

$$\frac{dN_i}{dt} = kR_i^{[1]} + R_i^{[2]} - kR_i^{[3]} - R_i^{[4]} \tag{30}$$

The k here is the volume correction factor. In what follows it is demonstrated that the rate of change of the total number of particles (the zero moment) is independent of k and, moreover, is predicted correctly by Eq. 30. It is then demonstrated that a constant value of $k = 2/3$ enables Eq. 30 to predict correctly the rate of change of total volume of particles.

The rate of change of the zero moment for the case of a size-independent kernel may be computed by the application of Eq. 24 to Eq. 30 with $\beta = \beta_0$:

$$\frac{dm_0}{dt} = \sum_i \frac{dN_i}{dt}$$

$$= \sum_i \sum_{j=1}^{i-1} k \cdot 3 \cdot 2^{j-i-1} \beta_0 N_i N_j + \sum_i \frac{1}{2} \beta_0 N_i^2$$

$$- \sum_i \sum_{j=1}^{i-1} k \cdot 3 \cdot 2^{j-i-1} \beta_0 N_i N_j$$

$$- \sum_i \sum_{j=i}^{\infty} \beta_0 N_i N_j$$

$$= \beta_0 \sum_i \left(\frac{1}{2} N_i^2 - N_i \sum_{j=i}^{\infty} N_j \right)$$

$$= -\frac{1}{2} \beta_0 \sum_i \left(N_i^2 + 2N_i \sum_{j=i+1}^{\infty} N_j \right)$$

$$= -\frac{1}{2} \beta_0 \sum_i N_i \sum_j N_j$$

$$= -\frac{1}{2} \beta_0 m_0^2$$

which is the required result, Eq. 20.

In a similar fashion, the rate of change of the third moment may be computed:

$$\frac{dm_3}{dt} = \sum_i \overline{L_i^3}\frac{dN_i}{dt}$$
$$= \sum_i \overline{L_{i+1}^3}\sum_{j=1}^{i-1} k \cdot 3 \cdot 2^{j-i}\beta_0 N_i N_j + \sum_i \frac{1}{2}\beta_0 \overline{L_{i+1}^3} N_i^2 - \sum_i \overline{L_i^3} \cdot \sum_{j=1}^{i-1} \cdot k \cdot 3 \cdot 2^{j-i-1}\beta_0 N_i N_j$$
$$- \sum_i \overline{L_i^3}\sum_j \beta_0 N_i N_j = \beta_0 \overline{L_i^3}\sum_i \cdot \left(N_i^2 + N_i \sum_{j=1}^{i-1} k \cdot 3 \cdot 2^{j-i-1} N_j - N_i \sum_j N_j\right)$$
$$= \beta_0 \overline{L_i^3}\sum_i \left(N_i \sum_{j=1}^{i-1} k \cdot 3 \cdot 2^{j-i-1} N_j - N_i \sum_{j=i+1}^{\infty} N_j\right)$$

if $k = 2/3$ the two terms inside the brackets of the last equation may be shown to be identical and we have $dm_3/dt = 0$. This again is the required result, Eq. 21. The reason for the inclusion of the volume correction factor, k, is now apparent. Its presence has no effect on the rate of change of total particle numbers, the zero moment, but its inclusion is essential if total particle volume is to be conserved during aggregation. The need for such a factor may be readily rationalized. In accounting for the birth or death of particles they are assumed to be added to, or removed from, a size interval uniformly, maintaining the stepped shape of Figure 1b. In fact, of course, a smooth distribution should develop. The volume correction factor allows for this inexact placement of numbers.

It can also be determined readily that k should only be applied to $R_i^{[3]}$ and $R_i^{[3]}$. When checking that crystal numbers decrease at the correct rate it is found that $R_i^{[2]}$ and $R_i^{[4]}$ cancel; moreover, $R_i^{[1]}$ and $R_i^{[3]}$ give exactly the right answer. There is no scope to modify these terms. The only course of action remaining is modification of $R_i^{[2]}$ and $R_i^{[4]}$, which is precisely the effect achieved by the application of the volume correction factor, k. It is remarkable indeed that k is a constant for all distributions.

The complete equation is

$$\frac{dN_i}{dt} = N_{i-1}\sum_{j=1}^{i-1} 2^{j-i+1}\beta_{i-1,j}N_j + \frac{1}{2}\beta_{i-1,i-1}N_{i-1}^2 - N_i\sum_{j=1}^{i-1} 2^{j-i}\beta_{i,j}N_j - N_i\sum_{j=i}^{\infty}\beta_{i,j}N_j \quad (31)$$

Testing the model

The aggregation terms of the population balance have now been expressed as a family of ordinary differential equations. These may be solved numerically using conventional techniques. A thorough check of this result would involve comparison with a number of analytical solutions to the original partial differential equation using as many initial conditions as possible. However, analytical solutions are seldom available when terms for aggregation are included; particularly for an arbitrary initial PSD.

Size-independent Coalescence Kernel. For the idealized case of an exponential PSD, as given by Eq. 32,

$$n_0' = \frac{N_0}{v_0}\exp(-v/v_0) \quad (32)$$

Gelbard and Seinfield (1978) provide a number of analytical solutions. For the simplest case of aggregation with a constant coalescence kernel they offer Eq. 33:

$$n' = \frac{4N_0}{v_0(\tau+2)^2}\exp\left(-\frac{2v/v_0}{\tau+2}\right) \quad (33)$$

where $\tau = N_0\beta_0 t$. Defining a dimensionless length and number as

$$\tilde{L}_i = \left(\frac{v_i}{v_0}\right)^{1/3} \quad \text{and} \quad \tilde{N}_i = \frac{N_i}{N_0} = \frac{1}{N_0}\int_{v_i}^{2v_i} n'\,dv$$

the analytical solution becomes

$$\tilde{N}_i = \frac{2}{\tau+2}\left[\exp\left(-\frac{2\tilde{L}_i^3}{\tau+2}\right) - \exp\left(-\frac{4\tilde{L}_i^3}{\tau+2}\right)\right] \quad (34)$$

The numerical solution of Eq. 31 is plotted along with the analytical solution from Eq. 34 in Figure 2. A greater degree of agreement could scarcely be hoped for. Given the ability of Eq. 34 to predict the dynamic PSD for this problem, it has to be expected that the moments inferred from the numerical solution will be in excellent agreement with those deduced analytically.

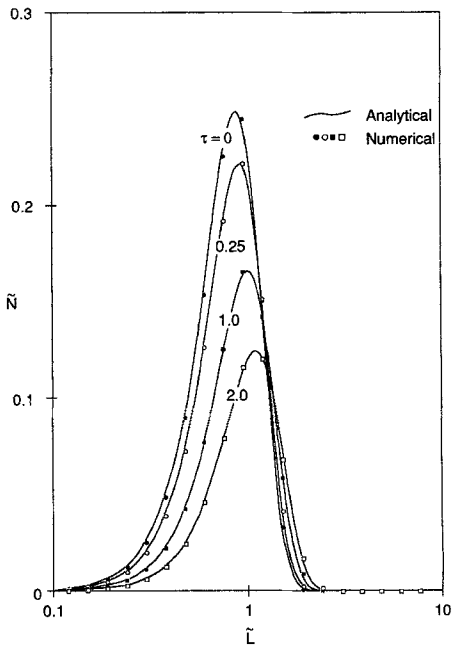

Figure 2. Comparison of analytical solution, Eq. 34, with Eq. 31 for aggregation, with a constant kernel, of an exponential distribution.

If the dimensionless moment is defined as

$$\tilde{m}_j = \frac{m_j}{m_j|_{t=0}}$$

Eq. 35 may be deduced from Eq. 33:

$$\tilde{m}_j = \left(\frac{2}{\tau + 2}\right)^{1-j/3} \tag{35}$$

In Figure 3 the analytical and numerical moments are compared. As has already been demonstrated, the zero and third moments are predicted exactly. Excellent agreement is also achieved for the first and second moments.

Size-dependent Coalescence Kernel. Before Eq. 31 can be claimed to describe aggregation in a general sense, it must be tested with a size-dependent coalescence kernel.

In addition to the size-independent result already quoted, Gelbard and Seinfeld produce a result for the aggregation of an exponential distribution with a kernel given by $\beta(u, v) = \beta_0(v + u)$, where v and u are the volumes of the colliding particles. The analytical solution for the population density function is

$$n' = \frac{N_0(1 - T)}{v\sqrt{T}} \exp\left[-(1 - T)\frac{v}{v_o}\right] I_1(2v\sqrt{T}) \tag{36}$$

where $T = 1 - e^{-\tau}$ and I_1 is the modified Bessel function of the first kind of order one. The nondimensional form of Eq. 36 is plotted in Figure 4 along with the numerical solution deduced from Eq. 31. Once more the degree of fit is very high.

In summary, Eq. 31 provides an excellent description of aggregation for both constant and size-dependent coalescence kernels. The equation is guaranteed to predict the zero and third moments correctly and has been seen to deal well with the intervening moments.

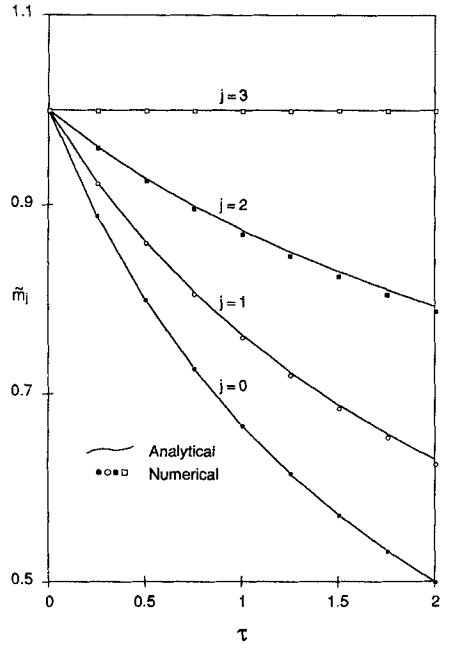

Figure 3. Predicted and analytical moments for aggregation of an exponential distribution.

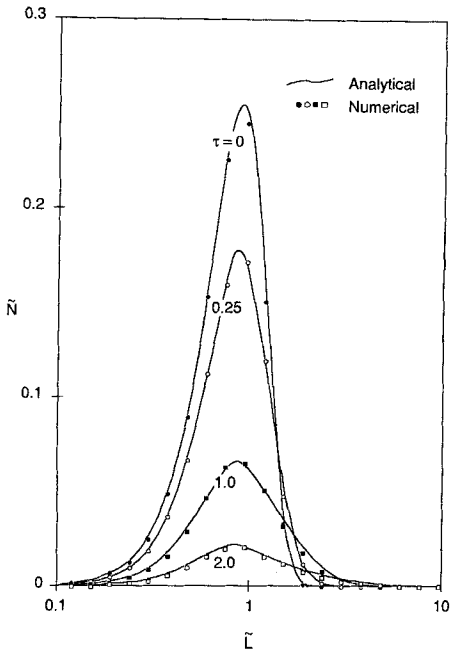

Figure 4. Comparison of analytical solution. Eq. 36, with Eq. 31 for aggregation of an exponential distribution, with $\beta = \beta_0(u + v)$.

Discretization for Growth

For growth alone the solution of Eq. 1 by conventional means is straightforward. However, the introduction of aggregation terms encourages the use of other techniques. If a technique similar to that presented earlier for aggregation is to be used, a discrete description of growth must be developed.

Previous work

The description of crystal growth requires the conversion of Eq. 2 to discrete form. If the particle size distribution is taken to be as shown in Figure 1a, with length as the internal coordinate, then in time dt a number of particles, dN_{in} will grow into the ith size range from the $(i - 1)$th size range:

$$dN_{in} = Gn(L_i)dt$$
$$= \frac{N_{i-1}}{L_i - L_{i-1}} Gdt$$

Similarly a number of particles will grow out of the ith interval into the $(i + 1)$th interval:

$$dN_{out} = \frac{N_i}{L_{i+1} - L_i} Gdt$$

The overall rate is given by

$$\frac{dN_i}{dt} = G\left(\frac{N_{i-1}}{L_i - L_{i-1}} - \frac{N_i}{L_{i+1} - L_i}\right)$$
$$= \frac{G}{(r-1)L_i}(rN_{i-1} - N_i) \qquad (37)$$

where r is the ratio of the upper and lower limits of size for any size interval

$$r = \frac{L_{i+1}}{L_i} \qquad (38)$$

All the examples considered here use a value of $r = \sqrt[3]{2}$.

In order to check the accuracy of Eq. 37 the rate of change of the moments it predicts may be calculated by the application of Eq. 24. In order to do so a relationship between L_i and $\overline{L_i^j}$ is required.

Assuming that the particle size distribution is as shown in Figure 1a, with length as the internal coordinate, it follows from Eq. 23 that

$$m_j = \sum_i \int_{L_i}^{L_{i+1}} L^j n\, dL$$
$$= \sum_i \int_{L_i}^{L_{i+1}} L^j \frac{N_i}{L_{i+1} - L_i} dL$$
$$= \sum_i \frac{N_i}{j+1}\left(\frac{r^{j+1} - 1}{r - 1}\right) L_i^j$$

Equating this last result with Eq. 23 leads to

$$\overline{L_i^j} = \frac{1}{j+1}\left(\frac{r^{j+1} - 1}{r - 1}\right) L_i^j$$

which is the desired relationship between L_i and $\overline{L_i^j}$. However, if a value of $r = \sqrt[3]{2}$ is used the following may be calculated.

$$\overline{L_i} = 1.130 L_i \quad \overline{L_i^2} = (1.132 L_i)^2 \quad \overline{L_i^3} = (1.135 L_i)^3$$

It seems reasonable to suggest that

$$\overline{L_i^j} = (1.130 L_i)^j = \left(\frac{1+r}{2} L_i\right)^j = \left(\frac{L_{i+1} + L_i}{2}\right)^j = (\overline{L_i})^j \qquad (39)$$

Turning now to the rate of change of moments implied by Eq. 37:

$$\frac{dm_j}{dt} = \sum_i \overline{L_i^j} \frac{dN_i}{dt}$$
$$= \sum_i \left(\frac{1+r}{2} L_i\right)^j \frac{G}{(r-1)L_i}(rN_{i-1} - N_i)$$
$$= \left(\frac{1+r}{2}\right)\frac{r^j - 1}{r - 1} G \sum_i N_i \left(L_i \frac{1+r}{2}\right)^{j-1}$$
$$= \left(\frac{1+r}{2}\right)\frac{r^j - 1}{r - 1} G m_{j-1} \qquad (40)$$

Comparing Eq. 40 with Eq. 10, it may be seen that the discrete approximation provided by Eq. 37 yields results high by a factor of:

$$\left(\frac{1+r}{2}\right)\frac{r^j - 1}{r - 1}\frac{1}{j} = 1.130 \ (j = 1)$$
$$= 1.277 \ (j = 2)$$
$$= 1.449 \ (j = 3)$$

In other words, Eq. 37 implies a rate of change of the third moment that is high by some 45%. There is a general dispersion of the predicted population distribution to larger sizes, resulting in the overprediction of all the moments to an unacceptable degree.

We may also consider the work of Marchal et al. (1988), who propose that the growth term be evaluated as

$$\frac{dN_i}{dt} = \frac{G}{2L_i}\left(\frac{r}{r-1} N_{i-1} - \frac{1}{r^2 - r} N_{i+1}\right) \qquad (41)$$

from which follows

$$\frac{dm_j}{dt} = \left(\frac{r+1}{r-1}\right)\left(r^j - \frac{1}{r^j}\right)\frac{G}{4} m_{j-1}$$

which, by comparison with Eq. 10 is in error by a factor of

$$\frac{1}{4j}\left(\frac{r+1}{r-1}\right)\left(r^j - \frac{1}{r^j}\right) = 1.013 \ (j = 1)$$
$$= 1.041 \ (j = 2)$$
$$= 1.087 \ (j = 3)$$

The rate of change of the third moment is overpredicted by some 9%.

A new approach—the model

The objective now is to develop an equation capable of describing the dynamic PSD and its moments.

As an alternative to Eqs. 37 and 39, consider an expression of the form

$$\frac{dN_i}{dt} = \frac{G}{L_i}(aN_{i-1} + bN_i + cN_{i+1}) \qquad (42)$$

where a, b, and c are constants, which may be chosen in order to predict correctly as many moments as possible. Applying Eq. 24,

$$\frac{dm_j}{dt} G \sum_i \left(\frac{1+r}{2}\right)^j L_i^{j-1}(aN_{i-1} + bN_i + cN_{i+1})$$
$$= G \sum_i \left(\frac{1+r}{2}\right)^j L_i^{j-1} N_i (ar^{j-1} + b + cr^{1-j})$$

Comparison with Eq. 10 reveals that the rate of change of the jth moment will be predicted correctly if

$$\left(\frac{1+r}{2}\right)(ar^{j-1} + b + cr^{1-j}) = j$$

Setting j to 0, 1, and 2 in the above generates three linear equations that may be solved for a, b, and c. Such a process yields:

$$a = \frac{2r}{(1+r)(r^2-1)} \quad b = \frac{2}{1+r} \quad c = \frac{-2r}{(1+r)(r^2-1)}$$

Equation 42 becomes

$$\frac{dN_i}{dt} = \frac{2G}{(1+r)L_i}\left(\frac{r}{r^2-1}N_{i-1} + N_i - \frac{r}{r^2-1}N_{i+1}\right) \quad (43)$$

Testing the model

Equation 43 is guaranteed to predict the zero, first, and second moments correctly, as this was the criterion used in its derivation. Further, the rate of change of the third moment predicted by this equation is high by only 1.8%.

As a test of Eq. 43, consider a simulation in which the exponential distribution given by Eq. 32 grows with a constant rate of linear growth. The analytical solution is

$$\tilde{N}_i = \begin{cases} 0 & \tilde{L}_i \le \tau \\ \exp\left[-(\tilde{L}_i - \tau)^3\right] - \exp\left[-(r\tilde{L}_i - \tau)^3\right] & \tilde{L}_i > \tau \end{cases} \quad (44)$$

where $\tau = Gt/L_0$ and L_0 is the size corresponding to v_0.

In Figure 5 the analytical solution is compared with the numerical solution from Eq. 43. The numerical approximation clearly allows a correct tracking of the mode and smallest particle sizes. Indeed the total dispersion about the analytical solution is small.

A fourth-order Runge-Kutta technique was used in the integration of Eq. 43. Over the range studied, no effect of step size could be determined. In order to perform the integration an additional constraint must be placed on the values of N_i. Direct application of Eq. 43 produces uncontrolled oscillation in the predicted values of N_i commencing in the smallest size ranges and propagating through the entire distribution. The oscillations appear to begin when the number of particles in the first interval has fallen to zero. For any system in which the initial size distribution is not identically zero, the simple device of replacing any negative value of N_i with zero provides the correct answer.

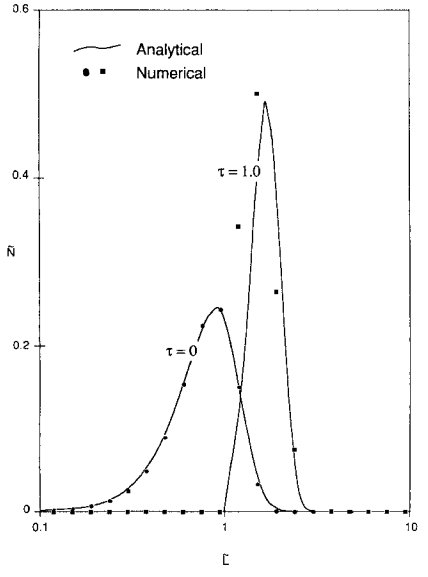

Figure 5. Analytical, Eq. 44, and numerical, Eq. 43, solutions for growth of an exponential distribution.

Discretization for Nucleation

The model

Nucleation is defined by Eq. 3 to occur at zero size. If the size domain is discretized into a sufficient number of intervals it is normally possible to allow nucleation to occur in the smallest size interval, in which case we may account for nucleation by

$$\frac{dN_1}{dt} = B_0 \quad (45)$$

To describe the usual phenomenon of simultaneous growth and nucleation, Eq. 45 need only be combined with Eq. 43. For unseeded systems this results in just the set of circumstances leading to oscillations in the PSD, that is, an identically zero size distribution.

The approach used in this work is to couple Eq. 45 with Eq. 37 for unseeded systems and to use Eq. 43 to describe growth for seeded systems. With a sufficient population of crystals Eq. 43 may be used, such as in the case study presented later.

Testing the model

For simultaneous nucleation and growth the population balance becomes

$$\frac{\partial n}{\partial t} = B_0\delta(L) - G\frac{\partial n}{\partial L}$$

which, for the case of unseeded crystallization with constant values of G and B_0, may be solved to give

$$n(L,t) = \frac{B_0}{G}u\left(t - \frac{L}{G}\right)$$

where u is the unit step function. It follows that the number of particles in the ith interval is

$$N_i = \begin{cases} \dfrac{\Delta L_i B_0}{G} & L_{i+1} \le tG \\ \dfrac{B_0(tG - L_i)}{G} & L_{i+1} \ge tG > L_i \\ 0 & L_i > tG \end{cases} \quad (46)$$

In Figure 6 a comparison is made between the exact solution of Eq. 46 and the solution of discretized Eqs. 45 and 37 for the case of constant growth rate (G = 0.5 length units per time) and constant nucleation rate (B_0 = 10,000 per unit volume per unit time) after 10 time units. The length domain is discretized into a $\sqrt[3]{2}$ progression starting with $L_1 = 2^{-10/3}$. The numerical solution is in good agreement with the exact solution provided L_i is not too near tG. The need for such a proviso is to be expected: some dispersion of numbers from small to large sizes is inevi-

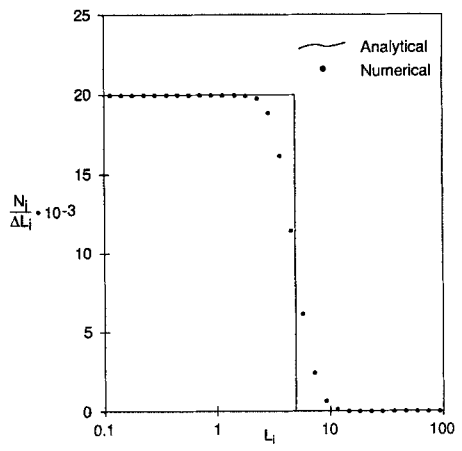

Figure 6. Analytical, Eq. 46, and numerical, Eqs. 37 and 45, solutions for unseeded nucleation and growth with $G = 0.5$, $B_0 = 10{,}000$.

tably associated with Eq. 37; further, a system of discretized equations cannot be expected to deal with an abrupt discontinuity in the discretized domain, particularly when the location of the discontinuity is not constant.

With reference to the analytical solution, Eq. 46, provided that L_{i+1} is less than tG the number of particles in each interval is constant at $N_i = \Delta L_i B_0/G$. The discretized equations predict exactly the same result. For the first interval the discretized equation is

$$\frac{dN_1}{dt} = B_0 - \frac{GN_1}{(\Delta)L_1}$$

Clearly no change in N_1 occurs when $N_1 = \Delta L_1 B_0/G$. Further, it may be shown that Eq. 37 implies $dN_i/dt = 0$ when $N_i = \Delta L_i B_0/G$. So, the discrete equations imply steady state at the same conditions as the exact solution. This result is displayed clearly in Figure 6.

The rate of change of moments implied by Eq. 45 will be in error as a consequence of introducing the nuclei at a finite size. In practice this error is insignificant.

Review of the Models

The main thrust of this work is the development of a simplification in the description of aggregation. Adopting the technique of discretization provides a simple set of ordinary differential equations that may be solved readily. The discretization developed here has the particular advantages that it correctly describes the rate of change of total particle number and volume and, for the systems tested, predicts the dynamic PSD with great precision.

If a population balance containing aggregation terms is to be solved using the new technique, similar discretizations must be developed for the other active mechanisms; in this case growth and nucleation. Nucleation may be dealt with expeditiously but growth presents some problems. The method chosen—allowing that the rate of change of particle numbers in interval i may be a function of the number of particles in that interval plus the two adjoining intervals, and choosing a form to satisfy the moment equations—produces a satisfactory result.

The combination of the equations for all three mechanisms produces a system of ordinary differential equations—Eqs. 31, 43, and 45—that not only predicts the rate of change of the moments correctly but describes the PSD with great accuracy.

Case Study—Batch Aggregation and Growth of Calcium Oxalate Monohydrate (COM)

Part of the research into the formation of urinary stones centers around the use of an *in vitro* batch crystallization technique in which COM seeds are added to a saline metastable calcium oxalate solution. The resulting growth and aggregation is followed with the aid of a particle size analyzer, such as a Coulter Counter. The details of this technique are documented extensively by Ryall et al. (1981).

As noted by Hartel and Randolph (1986), and again by Ryall et al. (1986), growth and aggregation into the field of view of the particle size analyzer has a significant impact on the shape of the PSD. To account for this, Hartel and Randolph introduce the notion of a source function, B_u. B_u is the rate of appearance of particles in the first size interval from the region of the particle size domain containing particles smaller than the minimum detectable by the particle size analyzer. Within the framework of a discretized size domain the source function is indistinguishable from the nucleation rate. Consequently, the analysis developed earlier for nucleation may be applied. Growth out of the field of view presents a much less significant problem when a particle size analyzer employing a geometric progression of size intervals is used.

The objective of the batch trials is to determine the effect on the rates of growth and aggregation of potentially inhibiting physicochemical factors. If a size-independent coalescence kernel and McCabe's ΔL law are assumed to apply, the growth and aggregation process may be simulated provided expressions can be deduced for the variation of the growth rate G, the kernel β_0, and the source function B_u, with supersaturation. Drach et al. (1978) produced a working definition of supersaturation for a system similar to that under consideration:

$$\Delta C = C_{ox} - C^*_{ox} \tag{47}$$

C^*_{ox}, the equilibrium oxalate concentration, may be calculated from the solubility product $C^*_{ox} = K_{sp}/\gamma^2_{\pm}C_{Ca}$. Finlayson (1977) describes appropriate techniques for the calculation of the terms of this expression. The instantaneous solute concentrations may be calculated from an oxalate balance.

Some results obtained for a set of control trials, in buffered saline metastable solution, are presented here. Particle size distributions were observed over the range 2 to 32 μm in a $\sqrt[3]{2}$ progression, corresponding to channels 5 to 16 on the Coulter counter. The first size distributions were measured at 10 min, with measurements repeated at 10 min intervals. Using the technique of Hounslow et al. (1988), the following kinetic relationships may be deduced.

$$\left.\begin{aligned} G &= 430\,\Delta C \\ \beta_0 &= 8.95\,\Delta C \end{aligned}\right\} \quad \text{first-order kinetics}$$

$$B_u = 1.53 \exp\left(-\frac{t}{13.1}\right)$$

The form of the expression given here for the source function, B_u, is entirely empirical but fits the experimental data well.

To simulate the growth and aggregation of the COM crystals, Eqs. 31, 43, and 45 are combined to yield a system of coupled ordinary differential equations, one equation for each channel simulated. For this example 13 channels are simulated, 12 corresponding to those of the Coulter counter plus one to allow the simulation of particles disappearing from the counter's field of view. The differential equations are solved using a fourth-order Runge-Kutta technique with the $t = 10$ min experimental data used as the initial conditions. No effect of integrator step size can be determined below $h = 10$ min. The simulation process takes typically less than 10 s on the range of micro- and superminicomputers tested.

The simulated and experimental moments are plotted in Figure 7. Two points are worthy of comment.

1. The shape of each curve: For systems in which growth occurs alone, the zero moment is constant and the higher moments increase with time, that is, there is no change in the number of particles but the volume of crystals increases. Conversely, in a system that undergoes only aggregation, the zero, first, and second moments all decrease, while the third moment remains constant; that is, the number of particles is reduced but the total volume remains constant. In this system a hybrid result is apparent: the zero and first moments decrease, the second moment remains relatively constant, and the third moment increases. Consequently the total area of crystal surface remains approximately constant.

2. The degree of agreement between the simulated and experimental results is excellent; in every case the trend and the magnitude of the changes with time are predicted. The assumptions of a size-independent growth rate and of a constant coalescence kernel are, at least provisionally, vindicated.

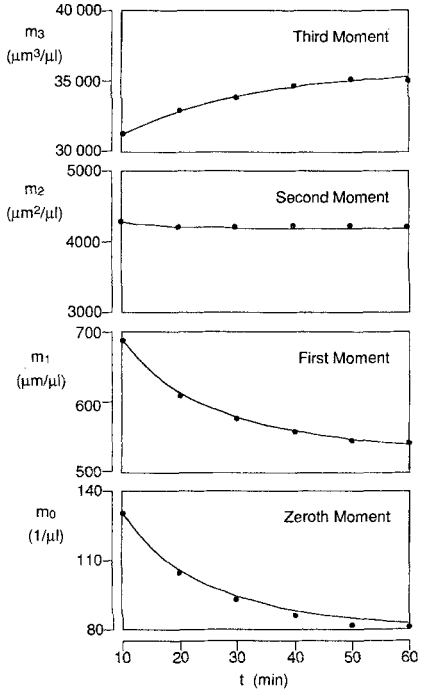

Figure 7. Experimental and simulated moments for batch growth and aggregation of COM crystals.

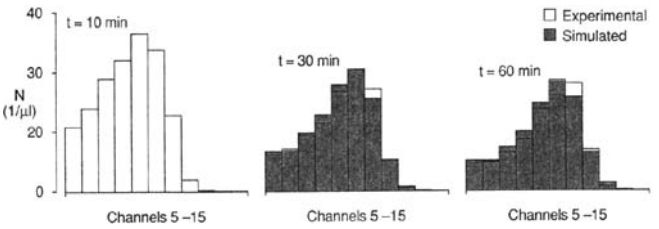

Figure 8. Experimental and simulated size distributions for batch growth and aggregation of COM crystals.

This argument is further strengthened by the comparison made in Figure 8 between the experimental and simulated particle size distributions. Again, both the shape and the magnitude of the experimental results are correctly predicted.

Conclusions

1. The population balance describing nucleation, growth, and aggregation of particles in constant-volume batch systems has been transformed from a partial differential integral equation into a set of ordinary differential equations. The equations have the desirable properties that they may be solved easily and rapidly, and use the same size discretization as a number of particle size analyzers.

2. The transformed equations produce results in close agreement with the analytical solutions tested for both size-independent and size-dependent coalescence kernels. Further, they correctly predict the rate of change of the first four moments of the particle size distribution.

3. The batch aggregation and growth of calcium oxalate monohydrate crystals are well described by McCabe's ΔL law, a size-independent coalescence kernel, and first-order kinetics. Simulated moments and particle size distributions are in excellent agreement with experimental results.

Acknowledgment

This work was supported by a project grant from the National Health and Medical Research Council of Australia and a grant in aid from the University of Adelaide. The authors thank C. M. Hibberd and R. M. Harnett for collecting the experimental data and W. R. Paterson for his detailed and incisive comments.

Notation

a, b, c = constants, Eq. 42
A_T = total crystal area per volume of suspension, $\mu m^2/\mu L$
B = birth rate, $1/\mu m \cdot \mu L \cdot min$
B_0 = nucleation rate, $1/\mu L \cdot min$
$\overline{B_j}, \overline{D_j}$ = birth and death terms, Eq. 11
C = solute concentration, mol/L
D = death rate, $1/\mu m \cdot \mu L \cdot min$
G = linear rate of growth, $\mu m/min$
h = integration step size, min
k = volume correction factor, Eq. 32
k_L, k_A, k_V = shape factors
K_{sp} = solubility product, mol^2/L^2
L = particle size
L_i = lower bound of ith size interval
$\overline{L_i}$ = mean size in interval i
L_T = total crystal length per volume of suspension, $\mu m/\mu L$

m_j = jth moment, $\mu m^j/\mu L$
n = population density function $1/\mu m \cdot \mu L$
N_0, v_0 = parameters, Eq. 32
N_i = number of particles in ith interval, $1/\mu L$
N_T = total crystal number per volume of suspension, $1/\mu L$
r = ratio L_{i+1}/L_i
R = rate of aggregation $1/\mu L \cdot$ min
t = time, min
u = unit step function
v = crystal volume, μm^3
V_T = total crystal volume per volume of suspension, $\mu m^3/\mu L$

Greek letters

β = coalescence kernel, $\mu L/min$
β_0 = size-independent portion of coalescence kernel, $\mu L/min$
δ = Dirac delta function
ΔC = supersaturation, mol/L
ΔL_i = ith size range, $L_{i+1} - L_i$, μm
ϵ = variable of integration, volume
τ = dimensionless time
$\gamma_\pm$ = activity coefficient
λ = variable of integration, length

Superscripts

$'$ = volume as internal coordinate
* = saturated condition
$\sim$ = dimensionless variable
[1], [2], [3], [4] = aggregation mechanisms, Table 1.

Subscripts

i, j = ith, and jth size intervals

Literature Cited

Batterham, R. J., J. S. Hall, and G. Barton, "Pelletizing Kinetics and Simulation of Full-Scale Balling Circuits," *Proc. 3rd Int. Symp. on Agglomeration,* Nürnberg, W. Germany, A136 (1981).

Drach, G. W., A. D. Randolph, and J. D. Miller, "Inhibition of Calcium Oxalate Dihydrate Crystallization by Chemical Modifiers. I: Pyrophosphate and Methylene Blue," *J. Urol.,* **119,** 99 (1978).

Finlayson, B., "Calcium Stones: Some Physical and Clinical Aspects," *Calcium Metabolism in Renal Failure and Nephrolithiasis,* D. S. David, ed, Wiley, New York (1977).

Gelbard, F., and J. H. Seinfield, "Numerical Solution of the Dynamic Equation for Particulate Systems," *J. Comp. Physics,* **28,** 357 (1978).

Hartel, R. W., and A. D. Randolph, "Mechanisms and Kinetic Modeling of Calcium Oxalate Crystal Aggregation in a Urinelike Liquor," *AIChE J.,* **32,** (7) 1186 (1986).

Hounslow, M. J., R. L. Ryall, and V. R. Marshall, "Modelling the Formation of Urinary Stones," *CHEMECA 88,* Sydney, Australia 1097 (1988).

Hulburt, H. M., and S. Katz, "Some Problems in Particle Technology. A Statistical Mechanical Formulation," *Chem. Eng. Sci.,* **19,** 555 (1964).

Kapur, P. C., and D. W. Fuerstenau, "A Coalescence Model for Granuation," *Ind. Eng. Chem. Process Des. Dev.,* **8,** (1), 56 (1969).

Marchal, P., R. David, J. P. Klein, and J. Villermaux, "Crystallization and Precipitation Engineering. I: An Efficient Method for Solving Population Balance in Crystallization with Agglomeration," *Chem. Eng. Sci,* **43**(1), 59 (1988).

McCabe, W. L., "Crystal Growth in Aqueous Solutions," *Ind. Eng. Chem.,* **21**(1), 30 (1929).

Ramkrishna, D., "The Status of Population Balances," *Rev. Chem. Eng.,* **3**(1), 49 (1985).

Randolph, A. D., and M. A. Larson, *Theory of Particulate Processes,* Academic Press, New York (1971).

Ryall, R. L., R. M. Harnett, and V. R. Marshall, "The Effect of Urine, Pyrophosphate, Citrate, Magnesium, and Glycosaminoglycans on the Growth and Aggregation of Calcium Oxalate Crystals *in vitro,*" *Clin. Chim. Acta.,* **112,** 349 (1981).

Ryall, R. G., R. L. Ryall, and V. R. Marshall, "A Computer Model for the Determination of Extents of Growth and Aggregation of Crystals from Changes in Their Size Distribution," *J. Crystal Growth,* **76,** 290 (1986).

Sastry, K. V. S., "Similarity Size Distribution of Agglomerates During Their Growth by Coalescence in Granulation or Green Pelletization," *Int. J. Miner. Process.,* **2,** 187, (1975).

Manuscript received Mar. 18, 1988, and revision received June 22, 1988.